

# Quintuple-period Si atomic wires with alternative double and triple modulations by metal: Mg/Si(557)

B.G. Shin <sup>a</sup>, M.K. Kim <sup>a</sup>, J.H. Lee <sup>a</sup>, D.-H. Oh <sup>a</sup>, I. Song <sup>a</sup>, S.H. Woo <sup>b</sup>, C.-Y. Park <sup>a,c</sup>, J.R. Ahn <sup>a,d,\*</sup>

<sup>a</sup> BK21 Physics Research Division, Sungkyunkwan University, Suwon 440-746, Republic of Korea

<sup>b</sup> College of Pharmacy, Chungnam National University, Daejeon 305-764, Republic of Korea

<sup>c</sup> Department of Energy Science, Sungkyunkwan University, Suwon 440-746, Republic of Korea

<sup>d</sup> SKKU Advanced Institute of Technology (SAINT), Sungkyunkwan University, Suwon 440-746, Republic of Korea

## ARTICLE INFO

### Article history:

Received 15 June 2011

Accepted 26 August 2011

Available online 5 September 2011

### Keywords:

Scanning tunneling microscopy

Vicinal Si surface

Atomic wire

Low energy electron diffraction

## ABSTRACT

The formation of Mg-induced quasi-one-dimensional atomic wires on a Si(557) surface was studied by low energy electron diffraction (LEED), scanning tunneling microscopy (STM), and first-principles calculations. The atomic wires were produced on the Si(557) surface without faceting when heated to 330 °C. The atomic wires had a  $\times 5$  period along the wires, as observed by LEED. STM images showed the existence of three kinds of atomic wires in a unit cell: an atomic wire located at the step edge and the others on the terrace. Interestingly, alternative double and triple modulations resulting in the  $\times 5$  period was observed at the atomic wire located at the step edge. Among the variety of atomic structure models available, the one based on a honeycomb-chain-channel model, which is that of a metal/Si(111)-(3 $\times$ 1) surface, reproduced the STM images well and was relatively stable energetically.

© 2011 Elsevier B.V. All rights reserved.

## 1. Introduction

Recently, vicinal Si(111) surfaces have been studied extensively to fabricate one-dimensional (1D) structures efficiently and to understand their underlying phenomena. Among the vicinal Si(111) surfaces, quasi-1D wires with a highly anisotropic electronic structure were first found on a Au/Si(557) surface [1–7]. A metallic Au/Si(553) surface with multiple quasi-1D metallic energy bands was discovered next [7–9]. The interesting quasi-1D metal-insulator transition, which was originally suggested to be due to quasi-1D charge density wave, is still under debate. An order–disorder transition and magnetic ordering were also suggested to be its origin [5,9–19]. More recently, quasi-1D transport and strong lateral coupling were observed on a Pb/Si(557) surface [20–22] and a triple-period atomic wire was reported on a In/Si(557) surface [23].

The reactions of alkali metals (AM) and alkaline earth metals (AEM) with surfaces have been studied as a fundamental reaction on both metal and semiconductor surfaces and many interesting phenomena in surface science have been reported [24–30,34]. On a Si(111) surface, one of intensively-studied systems was the metal(AM, AEM)-induced Si(111)-(3 $\times$ 1) surface with an anisotropic two-dimensional atomic structure [31–42,44–46]. Here, we report how the atomic structure of the Si(557) surface is reconstructed one-dimensionally by a metal with a simple electronic structure, where Mg was chosen as a prototype.

Interestingly, Mg produced quintuple-period Si atomic wires with alternative double and triple modulations, as shown in Fig. 1, maintaining the same terrace width as the bulk-terminated Si(557) surface, whereas only double and triple spacing have been observed. An atomic structure model with a honeycomb-chain-channel (HCC) structure, which was the building block of the metal/Si(111)-(3 $\times$ 1) surface, reproduced most of the features of the scanning tunneling microscopy (STM) images and was energetically stable compared to other atomic structure models [31,34,36,42,47–50,52]. Moreover, since most of the atomic structures of other metal-induced vicinal Si(111) surfaces were similar to the relaxed bulk-terminated Si(111) surfaces, it is interesting that two honeycomb chains separated by an empty channel can be stabilized on a Si(557) surface.

## 2. Methods

The experiments were performed in an ultrahigh vacuum chamber equipped with commercial variable-temperature STM (Omicron, Germany) and low energy electron diffraction (LEED) (Omicron, Germany). An *n*-type Si(557) wafer (9.45° offcut from the [111] orientation toward the [1 1 2] direction) was used. A clean Si(557) surface was prepared by repeated resistive heating, where an electric voltage was applied along the step edge direction [58,59]. Mg was evaporated by heating a tungsten wire wrapping a Mg rod. The Mg coverage of the Mg/Si(557)-(5 $\times$ 1) surface was approximately 0.2 ML, where the Mg coverage was roughly calibrated based on that of the Mg/Si(111)-(3 $\times$ 1) surface [43,44]. First-principles calculations were performed using VASP based on the density functional theory [60]. For the total

\* Corresponding author at: BK21 Physics Research Division, Sungkyunkwan University, Suwon 440-746, Republic of Korea. Tel.: + 82312905901; fax: + 82312907055.

E-mail address: [jrahn@skku.edu](mailto:jrahn@skku.edu) (J.R. Ahn).

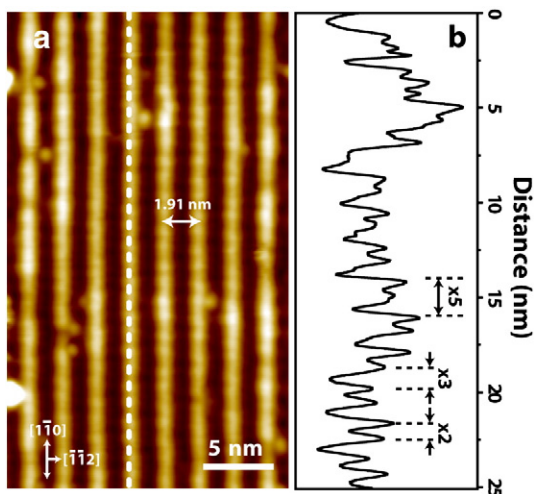


**Fig. 1.** (a) A filled-state STM image ( $V_s = -2.5$  V) of the Mg/Si(557)-(5 $\times$ 1) surface produced at  $T_s = 330$  °C. (b) The line profile along the dotted line in (a).

energy and force calculations, ultrasoft pseudopotentials provided with VASP were used within the generalized gradient approximation for the exchange-correlation energy [61,62]. The plane-wave cutoff energy was 250 eV. For surface Brillouin-zone integration, a  $2\times 2$  grid in Monkhorst-Pack special  $\vec{k}$ -point scheme including  $\Gamma$ -point was used [63]. The calculations were performed in a slab geometry with three Si bilayers and a vacuum region of approximately 18 Å. Si atoms at the bottom were saturated with H. All atomic positions were determined by minimizing the total energy until the residual forces on each atom were smaller than 0.04 eV/Å with the bottom Si and H layers kept fixed. STM images were simulated using the method reported by Tersoff and Hamann [64].

### 3. Results and discussion

#### 3.1. LEED and STM experiments

The phase transitions of the Si(557) surface were investigated as a function of temperature and Mg coverage by LEED. A (5 $\times$ 1) LEED pattern

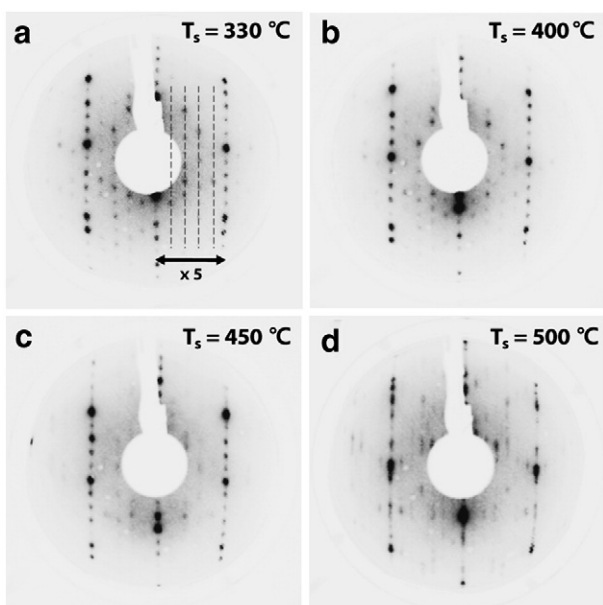


**Fig. 2.** LEED patterns of the Mg/Si(557)-(5 $\times$ 1) surface produced at  $T_s =$  (a) 330, (b) 400, (c) 450, and (d) 500 °C, respectively.

began to appear when the sample was heated to 300 °C, as shown in Fig. 2. The (5 $\times$ 1) LEED pattern was optimized at temperatures ranging from 300 to 400 °C. When heated to 450 °C, the (5 $\times$ 1) LEED pattern became blurred. The (5 $\times$ 1) LEED pattern disappeared and a (7 $\times$ 1) LEED pattern of the clean Si(557) surface reappeared when heated above 500 °C. STM images of the Mg/Si(557)-(5 $\times$ 1) surface [hereafter Mg-(5 $\times$ 1)] were acquired to understand its real space morphology. Fig. 3 shows filled-state STM images of the Mg-(5 $\times$ 1) surfaces produced at 330 and 400 °C, respectively. The Mg-(5 $\times$ 1) LEED patterns were similar in the temperature range from 330 to 400 °C. On the other hand, uniformity of the Mg-(5 $\times$ 1) surface was quite different in the STM images. When the temperature of the sample ( $T_s$ ) was near 330 °C, atomic wires were aligned uniformly with minimal atomic defects, as shown in Fig. 3(a)–(c). In contrast, when  $T_s \sim 400$  °C [see Fig. 3(d)–(g)], atomic and line defects developed, which might be due to Mg desorption.

The filled-state STM image of the Mg-(5 $\times$ 1) surface shows that the distance between the wires is 1.91 nm which is the same length of the single terrace of the bulk-terminated Si(557) surface, as shown in Fig. 1(a). The line profile along the wire shows that the  $\times 5$  period along the wire is made up of alternative double and triple modulations

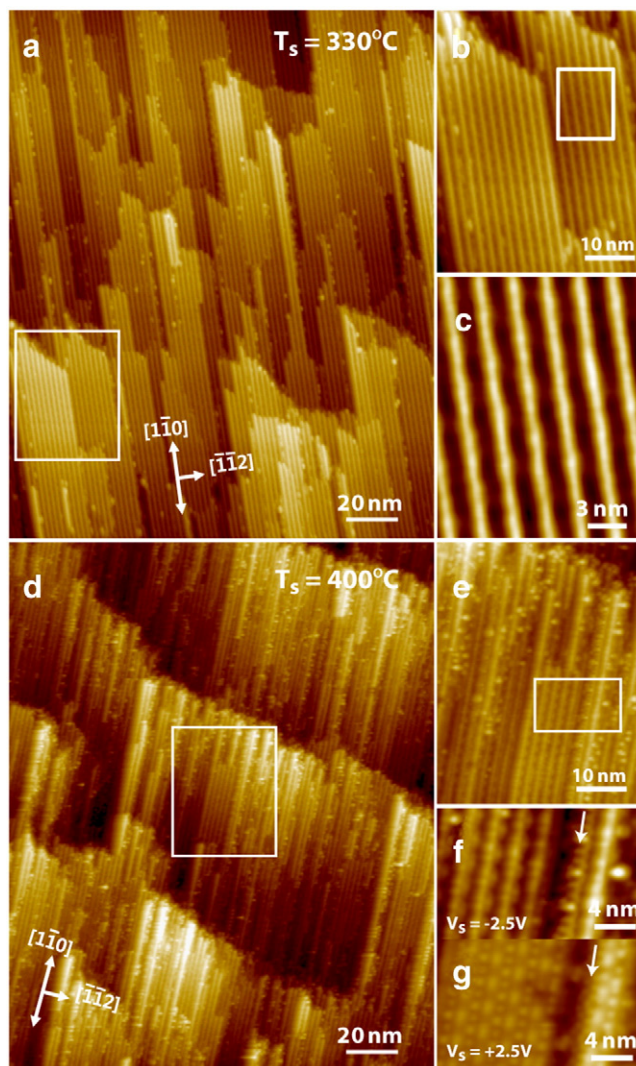


**Fig. 3.** Filled-state STM images ( $V_s = -2.5$  V) of the Mg/Si(557)-(5 $\times$ 1) surface produced at  $T_s =$  (a)–(c) 330 and (d)–(f) 400 °C, respectively. Panels (b) and (c) are the enlarged images of the regions outlined by the rectangles in (a) and (b), respectively. Panel (e) is the enlarged image of the region outlined by the rectangle in (d). Panels (f) and (g) are the enlarged filled- and empty-state STM images of the region outlined by the rectangle in (e). The arrows in (f) and (g) indicate a clean Si(557) surface.

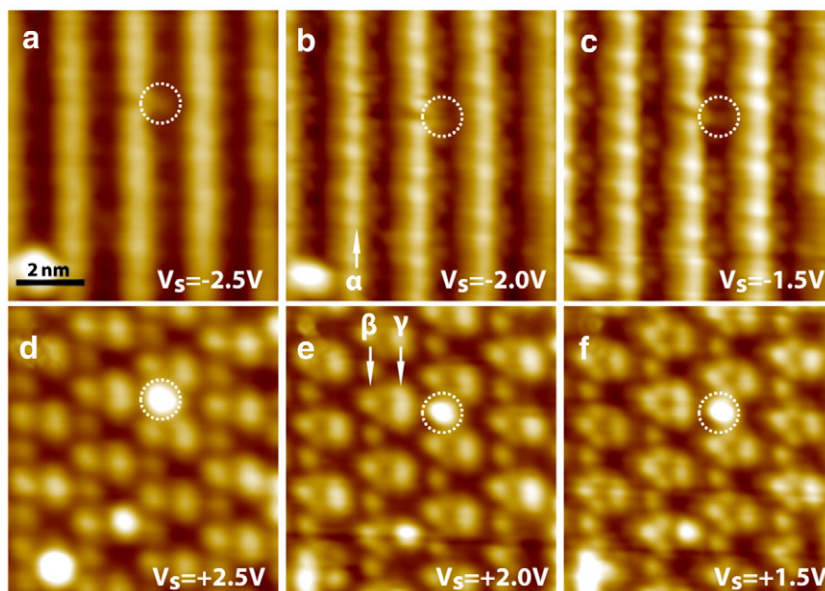


**Fig. 4.** (a)–(f) STM images of the Mg/Si(557)-(5 $\times$ 1) surface as a function of  $V_s$ .  $\alpha$ ,  $\beta$ , and  $\gamma$  indicate three representative chains in the STM images, respectively. Dotted circles indicate a defect which was used to determine the relative positions of the STM images with different  $V_s$ , s.

[see Fig. 1(b)]. Detailed morphology of the Mg-(5 $\times$ 1) surface was studied by changing bias voltage ( $V_s$ ), as shown in Fig. 4. The filled-state STM images [see Fig. 4(a)–(c)] were composed of a dominant bright line, which was denoted by the  $\alpha$  chain, with a weak modulation. In the empty-state STM images [see Fig. 4(d)–(f)], there are two types of 1D arrays of protrusions denoted by the  $\beta$  and  $\gamma$  chains, respectively. The  $\beta$  chain is a type of a zig-zag chain with different brightness, whereas the  $\gamma$  chain is a 1D array of an elliptical protrusion. The relative positions between the filled- and empty-state STM images were identified based on the atomic defect highlighted by dotted circles. Fig. 5 presents relative positions of the three chains more precisely, where Fig. 5(b) shows the line profiles along the three chains. The  $\alpha$  chain is made up of an alternative double and triple modulations, as described above. The height of the  $\beta$  chain is inversely proportional to that of the  $\alpha$

chain. The position of the  $\gamma$  chain with a maximum height is located at the same position of the  $\beta$  chain with a maximum height. The distance between the  $\alpha$  and  $\beta$  chains is 0.46 nm, while the distance between the  $\gamma$  and  $\alpha$  chains is 0.55 nm.

### 3.2. Atomic structure models

The underlying atomic structure of the STM images was investigated using first-principles calculations. Building up the atomic structure model using a completely different atomic structure from ones of the other Si surfaces is inefficient. Therefore, the cornerstones of the atomic structure models were based on the distinctive three chains of the STM images. First, the terrace width of the Mg-(5 $\times$ 1) surface has the same terrace width as the bulk-terminated Si(557) surface. Second, the  $\alpha$  chain with a weak modulation in the filled-state STM images was also observed on other metal-induced Si(557) surfaces [6,53]. On the Au/Si(557) [6] and In/Si(557) [23] surfaces, the  $\alpha$  chain was suggested to originate from a Si step edge structure. Third, the  $\beta$  and  $\gamma$  chains in the empty-state STM images become dark in the filled-state STM images. On the Si(111) surface, the AM- or AEM-induced surfaces show similar contrast in the filled- and empty-state STM images, where AM or AEM atoms were observed to be bright in the empty-state STM images particularly at a high  $V_s$  and be dark in the filled-state STM images [31,32,36,39,40,42,44,45,54–57]. Atomic structure models that were not based on the experimental clues were also examined but they did not reproduce the STM images and were energetically unstable.

Since the terrace width of the Mg-(5 $\times$ 1) surface is the same as the bulk-terminated Si(557) surface, the atomic structure models was based on the relaxed bulk-terminated Si(557) surface. In addition, the experimental clues suggest where Mg atoms are located from the Si step edge structure. The  $\beta$  chain is located near the  $\alpha$  chain originating from the Si step edge structure. This suggests that Mg atoms with a zig-zag adsorption site are located near the Si step edge structure, where the zig-zag adsorption site consists of the alternative two adsorption sites along the Si step edge structure. The zig-zag adsorption site reproduced the alternative double and triple modulations of the  $\alpha$  chain in the filled-state STM image, as shown in the simulated STM images in Fig. 6. The adsorption site also reproduced the reversed brightness of the  $\beta$  chain between the filled- and empty-state STM images and the zig-zag feature of the  $\beta$  chain with different

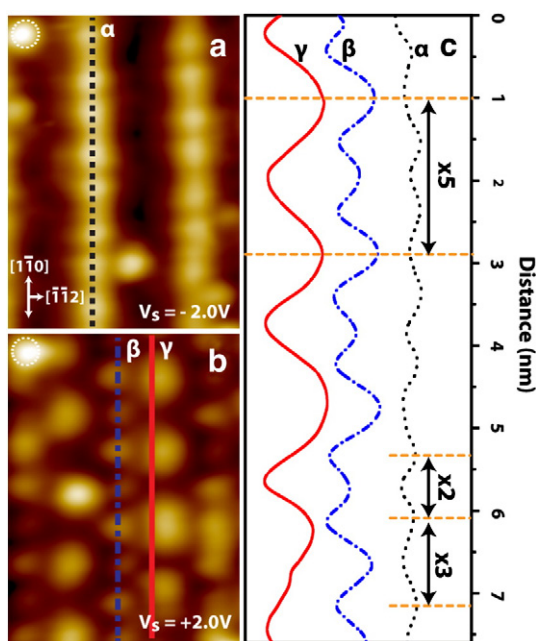


**Fig. 5.** (a) Filled- and (b) empty-state STM images of the Mg/Si(557)-(5 $\times$ 1) surface with  $V_s = -2.0$  and  $+2.0$  V, respectively. (c) Line profiles along the  $\alpha$ ,  $\beta$ , and  $\gamma$  chains in (a) and (b).

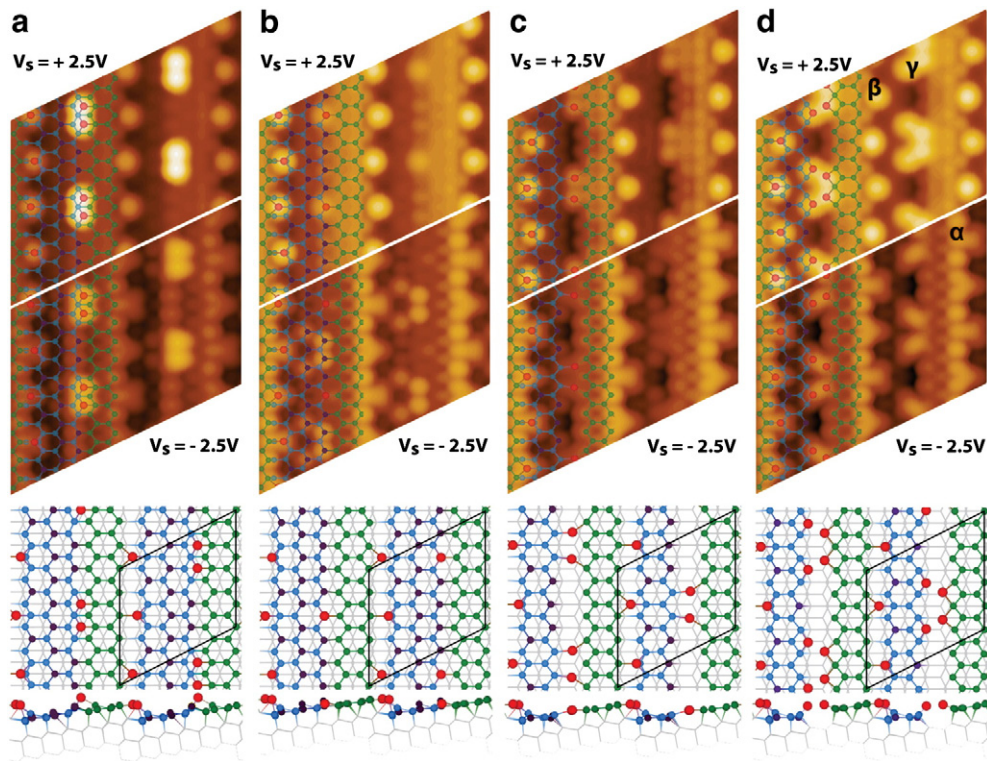


**Fig. 6.** (a)–(d) The simulated STM images and atomic structures of four representative models of the Mg/Si(557)-(5×1) surface: (a) overlayer, (b) substitution, (c) HCC, and (d) modified HCC models. The top and side views of atomic structure models are located at the bottoms of the simulated STM images and the top views of the atomic structure models overlap with the simulated STM images. Blue and red balls in the atomic structure models denote Si and Mg atoms, respectively. Especially, green and purple balls in the atomic structure models denote the Si atoms of the honeycomb chains and three-fold coordinated Si atoms in the terrace, respectively.

brightness in the empty-state STM image. On the other hand, the  $\gamma$  chain does not have a concrete basis compared to the  $\alpha$  and  $\beta$  chains.

The underlying atomic structure of the  $\gamma$  chain is related to the atomic structure within the terrace. Three representative atomic structure models were constructed based on the atomic structure models of other AM(or AEM)-adsorbed Si surfaces to better understand the  $\gamma$  chain: overlayer, substitution, and HCC models. Here, an atomic structure model based on the Seiwatz chain structure [40,51], which is one of AEM-adsorbed Si surfaces, was not considered. This is because when the Seiwatz chain was located within the terrace, its structure was very unstable energetically.

In the overlayer model, Mg dimers were located on the Si terrace, as shown in Fig. 6(a). The adsorption site was determined from the relative position of the  $\gamma$  chain to the  $\alpha$  chain in the STM image. The empty-state STM image was reproduced partially by the overlayer model but the filled-state STM image, particularly the  $\alpha$  chain, was not reproduced. Other overlayer structure models, such as a model with a Mg adatom, were also examined but the filled-state STM image was not reproduced even in the modified overlayer models. In the substitution model, the three-fold coordinated Si atoms in the Si topmost layer were substituted with Mg atoms, as shown in Fig. 6(b). The locations of the substituted Mg atoms were determined from the  $\gamma$  chain. Substituted Mg atoms in the simulated empty-state STM image did not show bright protrusions compared to the experimental STM image. The other substituted Mg sites also did not reproduce the empty-state STM image.

The HCC model consists of two Si honeycomb chains, where one is located at the Si step edge and another is located within the Si terrace, as shown in Fig. 6(c) and (d). On the AEM/Si(111)-(3×2) surface with the HCC structure, there are three favorable adsorption sites called  $T_4$ ,  $H_3$ , and  $B_2$ , respectively, where the  $T_4$  and  $H_3$  sites are almost degenerate energetically [36]. Fig. 6(c) shows an HCC model in which two Mg atoms are

located at the neighboring  $H_3$  sites on the empty channel. On the other hand, the structure did not show bright protrusions on the Mg sites in the simulated empty-state STM image, as shown in Fig. 6(c). A HCC model with a  $T_4$  Mg site was also similar to the HCC model with the  $H_3$  Mg site. The  $\gamma$  chain in the empty-state STM image consists of bright ellipses so that the single adsorption site on the HCC model is replaced by the successive adsorption site of  $H_3$  and  $T_4$ , as shown in Fig. 6(d). The modified HCC model reproduced the  $\gamma$  chain in the empty-state STM image as well as the  $\alpha$  chain in the filled-state STM image.

Among the various atomic structure models examined, only the modified HCC model reproduced most of the features in the STM images. A comparison of the simulated STM image with the experimental STM image is not enough to determine the underlying atomic structure. The energetic stability of the atomic structure models was thus further considered. The formation energy  $\Delta E_{form}$  is defined as  $\Delta E_{form} = (\Delta E_{total} - \mu_{Si}^{bulk} \Delta n_{Si} - \Delta \mu_{Si} \Delta n_{Si} - \mu_{Mg}^{bulk} \Delta n_{Mg} - \Delta \mu_{Mg} \Delta n_{Mg}) / A$ , where  $\Delta E_{total}$  is the total energy difference calculated by first-principles calculations,  $\mu_{Si}^{bulk}$  ( $\mu_{Mg}^{bulk}$ ) is the chemical potential of Si (Mg) in the bulk phase,  $\Delta n_{Si}$  ( $\Delta n_{Mg}$ ) is the change of the number of Si (Mg) atoms with respect to the bulk-terminated Si(557) surface.  $\Delta \mu_{Si}$  ( $\Delta \mu_{Mg}$ ) is a deviation from chemical potential of Si (Mg) in the bulk phase, where  $\Delta \mu_{Si}$  was set as  $-0.6$  eV for the Si atoms in the topmost layer [59], and  $A$  is the surface area of the Si(557)-(5×1) surface. Fig. 7 shows formation energies of four representative atomic structure models. The formation energies suggest that the overlayer and substitution models are more unstable compared to the HCC models. The two HCC models are energetically competitive with each other, where the relative stability depends on the chemical potential of Mg. Based on the simulated STM image and formation energy, the modified HCC model was found to be closest to the underlying atomic structure model.

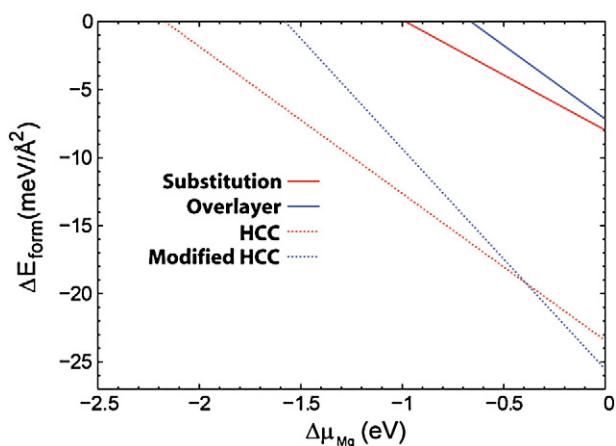


**Fig. 7.** The relative formation energies  $\Delta E_{form}$ 's of the atomic structure models of the Mg/Si(557)-(5 $\times$ 1) surface as a function of the relative chemical potential  $\Delta\mu_{Mg}$ . The  $\Delta E_{form}$ 's of substitution, overlayer, HCC, and modified HCC models are denoted by red solid, blue solid, red dotted, and blue dotted lines, respectively.

#### 4. Conclusions

The one-dimensional surface reconstructions of the Si(557) surface after Mg adsorption was investigated by LEED, STM, and first-principles calculations. The terrace width of the bulk-terminated Si(557) surface was maintained when the Mg/Si(557)-(5 $\times$ 1) surface was formed at 330 °C. STM images showed that the Mg/Si(557)-(5 $\times$ 1) surface is composed of three distinctive chains, called  $\alpha$ ,  $\beta$ , and  $\gamma$  chains. In addition, an interesting quintuple-period modulation with alternative double and triple modulations was observed at the  $\alpha$  chain. Atomic structure models were established based on the three chains in the STM images. Three representative structure models, overlayer, substitution, and HCC models, among various ones were discussed. Only the HCC model with a successive Mg adsorption site of  $H_3$  and  $T_4$ , reproduced most of the features of the three chains in the STM images. Moreover, the HCC model was energetically stable compared to the other atomic structure models. This leads to the conclusion that the quintuple modulation is induced by a zig-zag Mg adsorption site located near a Si step edge structure and the HCC model of a Mg-induced phase on a planar Si(111) surface can be stabilized on the Si(557) surface, which is a stepped Si(111) surface with a narrow terrace width.

#### Acknowledgements

This study was supported by the Korea Science and Engineering Foundation (KOSEF) grant funded by the Korea government (MEST) (No. 2009-0080512) and Priority Research Centers Program through the National Research Foundation of Korea (NRF) (2010-0029700) and the Converging Research Center Program through the Ministry of Education, Science and Technology (2011 K000611).

#### References

- [1] P. Segovia, D. Purdie, M. Hengsberger, Y. Baer, *Nature (London)* 402 (1999) 504.
- [2] R. Losio, K.N. Altmann, A. Kirakosian, J.-L. Lin, D.Y. Petrovykh, F.J. Himpsel, *Phys. Rev. Lett.* 86 (2001) 4632.
- [3] K.N. Altmann, J.N. Crain, A. Kirakosian, J.-L. Lin, D.Y. Petrovykh, F.J. Himpsel, R. Losio, *Phys. Rev. B* 64 (2001) 035406.
- [4] I.K. Robinson, P.A. Bennett, F.J. Himpsel, *Phys. Rev. Lett.* 88 (2002) 096104.
- [5] J.R. Ahn, H.W. Yeom, H.S. Yoon, I.-W. Lyo, *Phys. Rev. Lett.* 91 (2003) 196403.
- [6] H.W. Yeom, J.R. Ahn, H.S. Yoon, I.-W. Lyo, H. Jeong, S. Jeong, *Phys. Rev. B* 72 (2005) 035323.
- [7] J.N. Crain, A. Kirakosian, K.N. Altmann, C. Bromberger, S.C. Erwin, J.L. McChesney, J.-L. Lin, F.J. Himpsel, *Phys. Rev. Lett.* 90 (2003) 176805.
- [8] J.N. Crain, J.L. McChesney, F. Zheng, M.C. Gallagher, P.C. Snijders, M. Bissen, C. Gundelach, S.C. Erwin, F.J. Himpsel, *Phys. Rev. B* 69 (2004) 125401.
- [9] J.R. Ahn, P.G. Kang, K.D. Ryang, H.W. Yeom, *Phys. Rev. Lett.* 95 (2005) 196402.
- [10] P.C. Snijders, S. Rogge, H.H. Weitering, *Phys. Rev. Lett.* 96 (2006) 076801.
- [11] T.K. Rügheimer, Th. Fauster, F.J. Himpsel, *Phys. Rev. B* 75 (2007) 121401(R).
- [12] I. Barke, F. Zheng, T.K. Rügheimer, F.J. Himpsel, *Phys. Rev. Lett.* 97 (2006) 226405.
- [13] J.-H. Han, H.S. Kim, H.N. Hwang, B. Kim, S. Chung, J.W. Chung, C.C. Hwang, *Phys. Rev. B* 80 (2009) 241401(R).
- [14] H.S. Kim, S.Y. Shin, S.H. Uhm, C.C. Hwang, D.Y. Noh, J.W. Chung, *Phys. Rev. B* 80 (2009) 033412.
- [15] T. Okuda, K. Miyamoto, Y. Takeichi, H. Miyahara, M. Ogawa, A. Harasawa, A. Kimura, I. Matsuda, A. Kakizaki, T. Shishidou, T. Oguchi, *Phys. Rev. B* 82 (2010) 161410(R).
- [16] D. Sánchez-Portal, S. Riikonen, R.M. Martin, *Phys. Rev. Lett.* 93 (2004) 146803.
- [17] S. Riikonen, D. Sánchez-Portal, *Phys. Rev. B* 76 (2007) 035410.
- [18] S.C. Erwin, F.J. Himpsel, *Nat. Commun.* 1 (2010) 58.
- [19] P.C. Snijders, H.H. Weitering, *Rev. Mod. Phys.* 82 (2010) 307.
- [20] C. Tegenkamp, Z. Kallassy, H. Pfnür, H.-L. Günter, V. Zielasek, M. Henzler, *Phys. Rev. Lett.* 95 (2005) 176804.
- [21] K.S. Kim, H. Morikawa, W.H. Choi, H.W. Yeom, *Phys. Rev. Lett.* 99 (2007) 196804.
- [22] C. Tegenkamp, T. Ohta, J.L. McChesney, H. Dil, E. Rotenberg, H. Pfnür, K. Horn, *Phys. Rev. Lett.* 100 (2008) 076802.
- [23] I. Song, D.-H. Oh, J.H. Nam, M.K. Kim, C. Jeon, C.-Y. Park, S.H. Woo, J.R. Ahn, *New J. Phys.* 11 (2009) 063034.
- [24] H.P. Bonzel, A.M. Bradshaw, G. Ertl, *Physics and Chemistry of Alkali metal Adsorption*, Elsevier, Amsterdam, 1989.
- [25] S. Ciraci, I.P. Batra, *Phys. Rev. Lett.* 56 (1986) 877.
- [26] D. Heskett, T.M. Wong, A.J. Smith, W.R. Graham, N.J. DiNardo, E.W. Plummer, *J. Vac. Sci. Technol. B* 7 (1989) 915.
- [27] L.J. Whitman, J.A. Stroscio, R.A. Dragoset, R.J. Celotta, *Phys. Rev. Lett.* 66 (1991) 1338.
- [28] K. Wu, Y. Fujikawa, T. Nagao, Y. Hasegawa, K.S. Nakayama, Q.K. Xue, E.G. Wang, T. Briere, V. Kumar, Y. Kawazoe, S.B. Zhang, T. Sakurai, *Phys. Rev. Lett.* 91 (2003) 126101.
- [29] I.P. Batra, *Metallization and Metal-Semiconductor Interfaces*, NATO ASI Series B 195, Plenum, New York, 1989.
- [30] B. Reihl, R. Dudde, L.S.O. Johansson, K.O. Magnusson, *Appl. Phys. A* 55 (1992) 449.
- [31] S.C. Erwin, H.H. Weitering, *Phys. Rev. Lett.* 81 (1996) 2296.
- [32] M.-H. Kang, J.-H. Kang, S. Jeong, *Phys. Rev. B* 58 (1998) R13359.
- [33] L. Lottermoser, E. Landemark, D.-M. Smligies, M. Nielsen, R. Feidenhansl, G. Falkenberg, R.L. Johnson, M. Gierer, A.P. Seitsonen, H. Kleine, H. Bludau, H. Over, S.K. Kim, F. Jona, *Phys. Rev. Lett.* 80 (1998) 3980.
- [34] C. Battaglia, P. Aebi, S.C. Erwin, *Phys. Rev. B* 78 (2008) 075409.
- [35] C. Battaglia, H. Cercellier, C. Monney, L. Despont, M.G. Garnier, P. Aebi, *J. Phys. Conf. Ser.* 100 (2008) 052078.
- [36] S. Hong, G. Lee, H. Kim, *Surf. Sci.* 600 (2006) 3606.
- [37] K. Sakamoto, R.I.G. Uhrberg, *J. Surf. Sci. Nanotech.* 2 (2004) 210.
- [38] M. Gurnett, J.B. Gustafsson, L.J. Holleboom, K.O. Magnusson, S.M. Widstrand, L.S.O. Johansson, M.K.-J. Johansson, S.M. Gray, *Phys. Rev. B* 71 (2005) 195408.
- [39] A.A. Saranin, A.V. Zotov, V.G. Lifshits, M. Katayama, K. Oura, *Surf. Sci.* 426 (1999) 298.
- [40] A.A. Baski, S.C. Erwin, M.S. Turner, K.M. Jones, J.W. Dickinson, J.A. Carlisle, *Surf. Sci.* 476 (2001) 22.
- [41] K. Sakamoto, H.M. Zhang, R.I.G. Uhrberg, *Phys. Rev. B* 69 (2004) 125321.
- [42] R.H. Miwa, *Phys. Rev. B* 72 (2005) 085325.
- [43] J. Quinn, F. Jona, *Surf. Sci.* 249 (1991) L307.
- [44] O. Kubo, A.A. Saranin, A.V. Zotov, J.-T. Ryu, H. Tani, T. Harada, M. Katayama, V.G. Lifshits, K. Oura, *Surf. Sci.* 415 (1998) L971.
- [45] G. Lee, S. Hong, H. Kim, D. Shin, J.-Y. Koo, H.-I. Lee, D.W. Moon, *Phys. Rev. Lett.* 87 (2001) 056104.
- [46] T. Okuda, K.-S. An, A. Harasawa, T. Kinoshita, *Phys. Rev. B* 71 (2005) 085317.
- [47] C. Collazo-Davila, D. Grozea, L.D. Marks, *Phys. Rev. Lett.* 80 (1998) 1678.
- [48] M. Kuzmin, P. Laukkanen, R.E. Perälä, R.-L. Vaara, I.J. Väyrynen, *Phys. Rev. B* 71 (2005) 155334.
- [49] F. Palmino, E. Ehret, L. Mansour, J.-C. Labrune, G. Lee, H. Kim, J.-M. Themlin, *Phys. Rev. B* 67 (2003) 195413.
- [50] C. Eames, M.I.J. Probert, S.P. Tear, *Phys. Rev. B* 75 (2007) 205420.
- [51] F. Shimokoshi, I. Matsuda, S. Hasegawa, e-J. Surf. Sci. Nanotech. 2 (2004) 178.
- [52] N.D. Kim, T.S. Kang, J.H. Je, H.J. Kim, D.Y. Noh, J.W. Chung, *Appl. Phys. A* 91 (2008) 53.
- [53] M. Krawiec, T. Kwapiński, M. Jałochowski, *Phys. Rev. B* 73 (2006) 075415.
- [54] D. Jeon, T. Hashizume, T. Sakurai, R.F. Willis, *Phys. Rev. Lett.* 69 (1992) 1419.
- [55] S. Hasegawa, M. Maruyama, Y. Hirata, D. Abe, H. Nakashima, *Surf. Sci.* 405 (1998) L503.
- [56] A.A. Saranin, A.V. Zotov, V.G. Lifshits, J.-T. Ryu, O. Kubo, H. Tani, T. Harada, M. Katayama, K. Oura, *Phys. Rev. B* 58 (1998) 3545.
- [57] T. Sekiguchi, F. Shimokoshi, T. Nagao, S. Hasegawa, *Surf. Sci.* 493 (2001) 148.
- [58] A. Kirakosian, R. Bennewitz, J.N. Crain, Th. Fauster, J.-L. Lin, D.Y. Petrovykh, F.J. Himpsel, *Appl. Phys. Lett.* 79 (2001) 1608.
- [59] M.K. Kim, D.-H. Oh, J. Baik, C. Jeon, I. Song, J.H. Nam, S.H. Woo, C.-Y. Park, J.R. Ahn, *Phys. Rev. B* 81 (2010) 085312.
- [60] G. Kresse, J. Furthmüller, *Comput. Mat. Sci.* 6 (1996) 15.
- [61] D. Vanderbilt, *Phys. Rev. B* 41 (1990) 7892.
- [62] J.P. Perdew, J.A. Chevary, S.H. Vosko, K.A. Jackson, M.R. Pederson, D.J. Singh, C. Fiolhais, *Phys. Rev. B* 46 (1992) 6671 Phys. Rev. B 48 (1993) 4978.
- [63] H.J. Monkhorst, J.D. Pack, *Phys. Rev. B* 13 (1976) 5188.
- [64] J. Tersoff, D.R. Hamann, *Phys. Rev. B* 31 (1985) 805.